

## DMF, but not other fumarates, inhibits NF- $\kappa$ B activity in vitro in an Nrf2-independent manner



Geoffrey O. Gillard, Brian Collette, John Anderson, Jianhua Chao, Robert H. Scannevin, David J. Huss, Jason D. Fontenot\*

Biogen, Inc., 115 Broadway, Cambridge, MA 02142, USA

### ARTICLE INFO

#### Article history:

Received 19 February 2015

Received in revised form 7 April 2015

Accepted 9 April 2015

#### Keywords:

Dimethyl fumarate (DMF)

Monomethyl fumarate (MMF)

Monoethyl fumarate (MEF)

Nuclear factor kappa-light-chain-enhancer of activated B cells (NF- $\kappa$ B)

Nuclear factor (erythroid-derived 2)-like 2 (Nrf2)

Cytokine

### ABSTRACT

Fumarate-containing pharmaceuticals are potent therapeutic agents that influence multiple cellular pathways. Despite proven clinical efficacy, there is a significant lack of data that directly defines the molecular mechanisms of action of related, yet distinct fumarate compounds. We systematically compared the impact of dimethyl fumarate (DMF), monomethyl fumarate (MMF) and a mixture of monoethyl fumarate salts ( $\text{Ca}^{++}$ ,  $\text{Mg}^{++}$ ,  $\text{Zn}^{++}$ ; MEF) on defined cellular responses. We demonstrate that DMF inhibited NF- $\kappa$ B-driven cytokine production and nuclear translocation of p65 and p52 in an Nrf2-independent manner. Equivalent doses of MMF and MEF did not affect NF- $\kappa$ B signaling. These results highlight a key difference in the biological impact of related, yet distinct fumarate compounds.

© 2015 The Authors. Published by Elsevier B.V. This is an open access article under the CC BY-NC-ND license (<http://creativecommons.org/licenses/by-nc-nd/4.0/>).

### 1. Introduction

Fumarate esters, and particularly dimethyl fumarate (DMF), are approved therapeutics for the treatment of two major autoimmune pathologies – multiple sclerosis (MS) and psoriasis. Delayed-release DMF (also known as gastro-resistant DMF) is an approved oral therapeutic for the treatment of MS (Fox, 2012; Gold et al., 2012b; Kappos et al., 2008, 2012; Linker et al., 2011; MacManus et al., 2011). A mixture of DMF and three salt conjugates ( $\text{Ca}^{++}$ ,  $\text{Mg}^{++}$ , and  $\text{Zn}^{++}$ ) of monoethyl fumarate (MEF) (Hoefnagel et al., 2003) is an approved oral therapy for the treatment of psoriasis. Despite the demonstrable safety and efficacy of these therapeutics, the molecular mechanisms that underlie their efficacy have not been fully defined. Mechanism of action studies of the various fumarate esters [Table 1] have characterized anti-inflammatory, cytoprotective, and immunomodulatory properties (Fox et al., 2014; Linker and Gold, 2013; Linker et al., 2008; Moharreggh-Khiabani et al., 2009; Mrowietz and Asadullah, 2005). However, the unique and differential effects of these individual fumarate esters, as well as the major metabolite of DMF, monomethyl fumarate (MMF), remain largely unstudied.

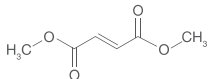
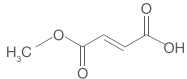
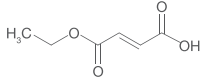
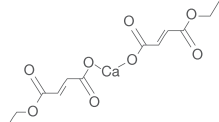
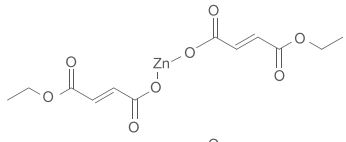
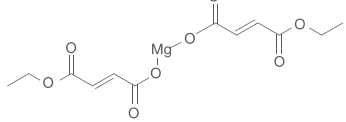
The majority of orally delivered DMF is rapidly metabolized to MMF by esterases in the intestine (Dibbert et al., 2013; Litjens et al., 2004c;

Werdenberg et al., 2003). Some DMF forms long-lived glutathione conjugates (Dibbert et al., 2013; Ghashghaeinia et al., 2010; Lehmann et al., 2007; Nelson et al., 1999; Rostami Yazdi and Mrowietz, 2008; Rostami-Yazdi et al., 2009; Schmidt and Dringen, 2010; Schmidt et al., 2007; Spencer et al., 1990). It is not clear precisely which cell populations and the degree to which different immunological compartments are directly exposed to significant levels of DMF or which cell populations and compartments are exposed exclusively to MMF and/or DMF-glutathione conjugates. Many preclinical studies have treated DMF and MMF as interchangeable, and not as two structurally related but distinct compounds. Although there have been fewer studies on the pharmacokinetic and pharmacodynamic properties of the MEF mixture as compared to DMF and MMF, the exposure levels of MEF and half-life in plasma are far more similar to those of MMF than DMF (Rostami-Yazdi et al., 2010).

There remains a significant lack of data that directly compares and defines the molecular mechanisms of action for these related yet distinct fumarate compounds and their contribution to the therapeutic effects of the pharmaceuticals that deliver them. The majority of in vitro and in vivo pre-clinical research has been conducted with DMF. In vivo, numerous studies have reported that DMF reduces the severity of experimental autoimmune encephalomyelitis (EAE), a mouse model of MS (Chen et al., 2014; Fox et al., 2014; Ghashghaeinia et al., 2010; Ghoreschi et al., 2011; Linker et al., 2011; Reick et al., 2014; Schilling et al., 2006). Four mechanisms of action have been described.

\* Corresponding author.

**Table 1**  
Chemical structures of fumarates tested.

Compound	Molecular formula	Molecular weight	Structure
DMF	C <sub>6</sub> H <sub>8</sub> O <sub>4</sub>	144.13	
MMF	C <sub>5</sub> H <sub>6</sub> O <sub>4</sub>	130.10	
MEF	C <sub>6</sub> H <sub>8</sub> O <sub>4</sub>	144.13	
MEF-calcium	C <sub>12</sub> H <sub>14</sub> CaO <sub>8</sub>	326.31	
MEF-zinc	C <sub>12</sub> H <sub>14</sub> O <sub>8</sub> Zn	351.62	
MEF-magnesium	C <sub>12</sub> H <sub>14</sub> MgO <sub>8</sub>	310.54	

First, DMF stimulates cytoprotective and anti-inflammatory responses via activation of the nuclear factor (erythroid-derived 2)-like 2 (Nrf2)-dependent anti-oxidant response pathway (Gold et al., 2012b; Linker et al., 2011; Scannevin et al., 2012; Wilms et al., 2010). Second, DMF inhibits nuclear factor kappa-light-chain-enhancer of activated B cells (NF-κB)-driven processes (Gerdes et al., 2007; Ghoreschi et al., 2011; Litjens et al., 2004b; Loewe et al., 2001, 2002; Moharreh-Khiabani et al., 2009; Mrowietz and Asadullah, 2005; Peng et al., 2012; Rostami-Yazdi and Mrowietz, 2008; Vandermeeren et al., 1997, 2001), resulting in downstream reduction in inflammatory cytokine production, altered maturation and function of antigen-presenting cells, and immune deviation of T helper cells (Th) from the Th1 and Th17 profile to a Th2 phenotype (Ghoreschi et al., 2011; Litjens et al., 2006; Moed et al., 2004; Peng et al., 2012; Peterson et al., 1998). Third, as an α, β carboxylic acid ester, DMF can bind thiol groups and modulate glutathione availability and production, which impacts cellular responses to oxidative stress (Dibbert et al., 2013; Lehmann et al., 2007; Murphy et al., 2001; Nelson et al., 1999; Peterson et al., 1998; Rostami-Yazdi and Mrowietz, 2008; Rostami-Yazdi et al., 2009; Scannevin et al., 2012; Schmidt and Dringen, 2010; Schmidt et al., 2007; Spencer et al., 1990). Fourth, agonism of G-protein coupled receptor 109A (GPR109A, also known as the hydroxycarboxylic acid receptor 2 (HCA2)) by DMF and MMF reduces neutrophil adhesion, migration, and recruitment to the CNS during EAE (Chen et al., 2014; Digby et al., 2012; Hanson et al., 2010, 2012; Rahman et al., 2014; Tang et al., 2008). The protective effect of DMF in EAE was mostly lost in HCA2-deficient mice (Chen et al., 2014).

While DMF has been the primary fumarate used in most mechanism of action studies, it has been assumed that MMF, as the primary *in vivo* metabolite, mediates all the mechanistic effects of DMF. However, the relationship between the mechanisms of action of DMF and MMF may not be so simple. For example, DMF but not MMF was shown to protect primary cortical cultures from oxidative glutamate toxicity (Albrecht et al., 2012). In another study, DMF was shown to be more potent than MMF in inducing Nrf2 activation (Scannevin et al., 2012). These examples challenge the assumption that DMF and MMF have identical function. As previously mentioned, much less is known about the

impact of the MEF mixture or the individual MEF salts on these biological processes. Despite reported similarities, a direct assessment on the effect and potency of DMF, MMF, and MEF has not been performed.

Given the clinical efficacy and safety of delayed-release DMF (Fox et al., 2012; Gold et al., 2012a) in treating MS and a mixture of DMF and MEF salts (Mrowietz and Asadullah, 2005; Roll et al., 2007) in treating psoriasis, there is significant interest in developing next-generation fumarate compounds and expanding the use of fumarates to new clinical indications where the multi-faceted mechanism of action may provide clinical benefit. Thus, this study was designed to systematically assess and compare the ability of various fumarates to modulate defined cellular responses.

## 2. Materials and methods

### 2.1. Screening in BioMAP model systems

#### 2.1.1. BioMAP assays

DMF and MMF were evaluated over a range of concentrations in a panel of *in vitro* systems to generate compound activity profiles using the BioMAP® platform (assays and analysis provided by BioSeek, Inc.) as described (Berg et al., 2010; Kunkel et al., 2004a,b). Compounds were tested at the indicated concentrations (DMF: 0.617, 1.852, 5.556, 16.7, 50, and 150 μM; MMF: 1.852, 5.556, 16.7, 50, 150 and 450 μM). Compounds were prepared in the solvent (DMSO) as directed, added 1 h before stimulation of the cells, and were present during the whole 24 hour stimulation period. The final concentration of solvent was 0.1% or less.

#### 2.1.2. Data analysis

BioMAP® profiles generated for DMF and MMF at nontoxic concentrations (16.7 and 50 μM for DMF, 50 and 150 μM for MMF) were compared and correlated to profiles of benchmark compounds in the BioSeek library. Assay details and statistics were as described previously (Berg et al., 2006; Kunkel et al., 2004b).

Mean OD values for each parameter were calculated from triplicate samples per experiment.

For the Benchmark Database comparisons, Pearson correlation coefficients were calculated between test compounds (at non-toxic, active

doses) and compounds from BioSeek's database (3C, 4H, LPS and SAg systems). Statistically significant correlations were identified based on comparisons of these true Pearson correlations to a set of Pearson correlations obtained from randomizing the experimentally observed values.

## 2.2. HCS screening of translocation of p65 and p52

### 2.2.1. Reference compound validation of assay

The reference compound for TNF-induced p65 nuclear translocation is 2-Amino-6-[2-(cyclopropylmethoxy)-6-hydroxyphenyl]-4-(4-piperidinyl)-3-pyridinecarbonitrile (ACHP), a commercially available IKK $\beta$  Inhibitor (Tocris Bioscience, Bristol, UK). The p52 translocation assay was validated using BIO-032202, an in-house reference compound based on a competitor's patented compound. All IC<sub>50</sub> curves for ACHP and BIO-032202 met acceptance criteria.

### 2.2.2. Dilution of fumarates

Compounds were added to the cells 30 min before stimulation. Eight doses of the fumaric acid esters (DMF, MMF, and MEF) were tested: 18, 12, 6, 3, 1, 0.5, 0.25, and 0.125  $\mu$ g/mL. In plates 3 and 4, dose-response curves were tested in the presence of 3  $\mu$ g/mL DMF or MMF.

### 2.2.3. Stimulation and assessment of p65 and p52 translocation

U-2 OS cells were stimulated with 10 ng/mL TNF- $\alpha$  for 30 min (p65 assay) or 10 ng/mL of the anti-lymphotoxin  $\beta$  receptor (LT $\beta$ R) antibody BS-1 for 4 h (p52 assay). The cells were then fixed and stained with an antibody that recognizes the appropriate protein. Images of each well were acquired on the PerkinElmer Operetta and the images were analyzed using PerkinElmer Columbus Image Analysis software. All plates had a Z' score  $\geq$  0.5 and a signal-to-noise ratio of  $\geq$  5.

## 2.3. Ramos-Blue reporter assay

### 2.3.1. Culturing Ramos-Blue B lymphocyte cell line

Ramos-Blue cells were thawed from the manufacturer (InvivoGen) and cultured in Ramos-Blue cell culture medium without the selective antibiotic Zeocin. The cells were then passaged every 3–4 days in the Ramos-blue cell culture medium with Zeocin at 100  $\mu$ g/mL to a concentration of  $1 \times 10^6$  cells/mL, and never exceeding  $6 \times 10^6$  cells/mL.

### 2.3.2. Dilution of DMF, MMF, and MEF

Compounds were prepared on a plate in DMSO at 15  $\mu$ g/mL and sequentially diluted in order to generate the different fumarate stock concentrations in a standard volume of DMSO. This dilution plate was used to make the final dilution of  $5 \times$  compound in Ramos-blue cell culture media. This was done by adding 3  $\mu$ l from each well (concentration) of the dilution plate to a 1.7 mL microcentrifuge tube containing 997  $\mu$ l of cell culture media.

### 2.3.3. Pre-incubation of Ramos-Blue cells with DMF, MMF, and MEF

Ramos-blue cells were re-suspended in Ramos-Blue culture medium without Zeocin at a concentration of  $2 \times 10^6$  cells/mL. 175  $\mu$ l of cells was added to the appropriate number of wells in a 96-well round bottom plate. The wells were treated with 50  $\mu$ l of the varying concentrations of each compound from the dilution tubes. The wells were incubated for 30 min at 37 °C and 5% CO<sub>2</sub>.

### 2.3.4. Activation of Ramos-Blue cells

Wells were treated with 25  $\mu$ l of ODN 2006 at a final working concentration of 10  $\mu$ g/mL. For CD40-stimulated cells, agonistic anti-human CD40 antibody clone G28.5 (Biolegend, Ultra-LEAF  $\alpha$ CD40) was added to a final working concentration of 10  $\mu$ g/mL. Isotype control antibody (BioLegend; Ultra-LEAF mouse IgG1  $\kappa$ , clone MOPC-21) was used at equal concentration for unstimulated wells. The wells were incubated for 24 h at 37 °C and 5% CO<sub>2</sub>.

### 2.3.5. Detection of NF- $\kappa$ B activity through the production of secreted embryonic alkaline phosphatase (SEAP)

The plate was centrifuged at 1800 rpm for 10 min to pellet cells. 40  $\mu$ l of supernatant was taken from the wells and put into a new 96-well flat bottom plate. 200  $\mu$ l of QUANTI-Blue reaction mixture, pre-warmed to 37 °C, was added to the wells. The wells were incubated at 37 °C for 75 min in the dark. The wells were read on a microplate reader using a wavelength of 635 nm.

## 2.4. Cytokine responses in fumarate-treated primary splenocytes in response to lipopolysaccharide (LPS) or CpG-B stimulation

### 2.4.1. Preparation of splenocytes

Primary splenocytes were isolated from age-matched NRF2<sup>-/-</sup> mice or age-matched control wild-type (WT) mice. Splenocytes were recovered via mechanical dissociation of spleens, followed by washing and lysis of RBS (Sigma). Cells were then counted, centrifuged, and resuspended at  $2 \times 10^6$  cells/mL in X-VIVO 10 (Lonza) chemically defined media and stored on ice.

### 2.4.2. Preparation of fumarate dilutions and working stocks

Stocks of fumarates for dilution series were at an initial concentration of 30 mg/mL in DMSO. Final concentrations to be tested were 9  $\mu$ g/mL, 6  $\mu$ g/mL, 3  $\mu$ g/mL, and 1  $\mu$ g/mL. Working stocks (4 $\times$  final concentration) of fumarates were generated in X-VIVO 10 media and mixed well.

### 2.4.3. Preparations of working stocks of LPS, CpG-B ODN 2006, CpG-B ODN 1826, and controls

Stocks of LPS (Sigma-Aldrich, ion-exchange chromatography purified from *Escherichia coli* strain 0111:B4) and CpG-B oligonucleotides (1826 for murine cell stimulation and 2006 for human PBMC stimulation; InvivoGen, San Diego, CA) were prepared at 40 ng/mL and 40  $\mu$ g/mL, respectively, in X-VIVO 10 media, to yield final concentrations of 10 ng/mL and 10  $\mu$ g/mL, respectively; 2 replicates per condition with no stimulation (vehicle control for each fumarate condition). Wells receiving vehicle (PBS) received 6  $\mu$ g/mL (final concentration) of fumarates.

### 2.4.4. Preparation of plates

For each plate, 50  $\mu$ l of fumarate/DMSO control working stock were added, followed by 50  $\mu$ l of stimulation mix, followed by 100  $\mu$ l of cells at  $2 \times 10^6$  cells/mL. Combination of working stocks and cells in final volume of 200  $\mu$ l/well result in the desired final concentrations of fumarates (9, 6, 3, 1, 0  $\mu$ g/mL) and stimuli (10 ng/mL for LPS and 10  $\mu$ g/mL for CpGs). Plates (2 plates per stimulus) were then transferred into 37 °C incubator and supernatants were harvested 24 h later and transferred to new 96 well plates that were immediately placed in -80 °C.

### 2.4.5. Quantification of cytokine/chemokine in cell culture supernatants

The Milliplex Magnetic multiplex mouse cytokine/chemokine magnetic premixed bead immunoassay (premixed 25-plex; Cat # MCYTOMAG-70 K-PMX) was used to quantify cytokine levels in tissue culture supernatants in direct accordance with the manufacturer's protocol. Freshly thawed tissue culture supernatant (25  $\mu$ l) was assayed in duplicate. All plates were run with overnight incubation of sample and beads at 4 °C with shaking. After washing and resuspension, beads were read on either a Luminex 100 reader or a Luminex 200 reader.

## 3. Results

### 3.1. DMF and MMF show significant overlap in activity profiles in BioMAP assays but marked differences in potency

Given that numerous cellular pathways are affected by fumarates, we began our study with a systematic screen for similarities and



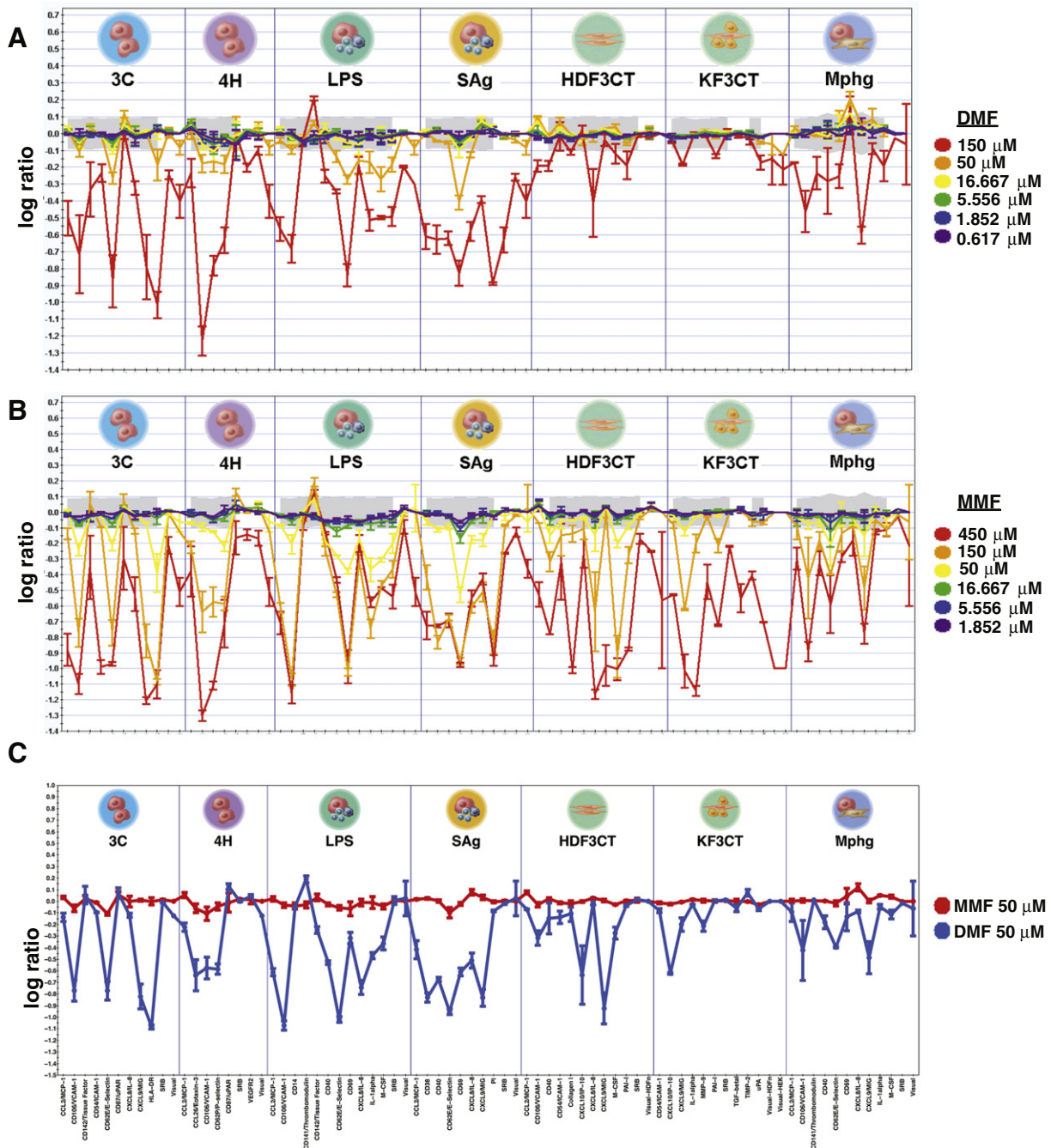


**Fig. 1.** BioMAP profiles for DMF and MMF. BioMAP profiles of DMF (A) and MMF (B), tested at multiple concentrations in 7 BioMAP systems. The biomarker readouts measured (see the Materials and methods section) are indicated along the x-axis. The y-axis shows the log<sub>10</sub> expression ratios of the readout level measurements relative to solvent (DMSO buffer) controls. Each datapoint represents a single well. The gray area above and below the dashed line indicates the 95% significance envelope of DMSO negative controls. The BioMAP profiles for DMF and MMF at a standard concentration of 50 mM are plotted in C.

differences between DMF and MMF using the BioMAP® system. The BioMAP® analysis system consists of 7 individual assays that use complex co-cultures of primary human cells to model the effects of tested

**Table 2**  
Reproducibility between two repeat BioMAP experiments.

Compound	Dose	Pearson correlation across seven BioMAP systems
DMF	150 μM (toxic)	0.87
DMF	50 μM	0.95
DMF	16.7 μM	0.86
MMF	450 μM (toxic)	0.93
MMF	150 μM	0.83

compounds on cell intrinsic-responses and diverse cell–cell interactions (Kunkel et al., 2004a,b). The effects of tested compounds are read out using multiple parameters for each of the seven assays. Additional details on the seven individual assays and the readouts for each assay can be found in Supplemental Table 1. The combined biological effects of a compound on each analyte in each assay are used to generate an activity profile for the compound. The activity profile of a compound observed in BioMAP® systems can be used to identify molecules and pathways that are affected by a given compound, and can also be compared (“benchmark”) against a database of activity profiles of hundreds of experimental drugs and approved therapeutics. This “benchmarking” provides insight into the mechanism of action or

**Table 3**  
Benchmarking hits in BioSeek database identify DMF and MMF as NF- $\kappa$ B-pathway modulators. DMF and MMF profiles at non-toxic doses were compared to profiles in the BioSeek Benchmark Database as described in Appendix 1. Compounds with significantly related profiles (FDR < 0.05) are listed. The correlation coefficients ( $r$ ) for the pairwise comparisons are shown for all four systems, and for individual systems.

Compound	Database Match	Mechanism	$r$	FDR	$r$ (individual systems)			
					LPS	3C	SAG	4H
DMF (50 $\mu$ M)	Ro106-9920 (5.5 $\mu$ M)	I $\kappa$ B $\alpha$ ubiquitination inhibitor	0.820	0.012	0.960	0.926	0.362	0.936
	BAY 11-7085 (2.7 $\mu$ M)	I $\kappa$ B $\alpha$ phosphorylation inhibitor	0.782	0.012	0.954	0.900	0.569	0.852
	Parthenolide (3.7 $\mu$ M)	NF- $\kappa$ B inhibitor (p65 alkylation)	0.768	0.012	0.755	0.950	0.500	0.664
	GW8510 (8.3 $\mu$ M)	CDK inhibitor	0.805	0.014	0.936	0.772	0.884	0.988
	Roscovitine (25 $\mu$ M)	CDK inhibitor	0.666	0.063	0.669	0.766	0.312	0.915
DMF (16.7 $\mu$ M)	Ro106-9920 (1.8 $\mu$ M)	I $\kappa$ B $\alpha$ ubiquitination inhibitor	0.847	0.009	0.852	0.726	0.874	0.973
	Ro106-9920 (5.5 $\mu$ M)	I $\kappa$ B $\alpha$ ubiquitination inhibitor	0.773	0.012	0.546	0.958	0.893	0.968
	BAY 11-7085 (0.9 $\mu$ M)	I $\kappa$ B $\alpha$ phosphorylation inhibitor	0.842	0.009	0.860	0.801	0.973	0.713
	BAY 11-7085 (2.7 $\mu$ M)	I $\kappa$ B $\alpha$ phosphorylation inhibitor	0.833	0.009	0.694	0.983	0.964	0.902
	Parthenolide (3.7 $\mu$ M)	NF- $\kappa$ B inhibitor (p65 alkylation)	0.781	0.012	0.691	0.778	0.932	0.886
MMF (150 $\mu$ M)	Roscovitine (8.3 $\mu$ M)	CDK inhibitor	0.702	0.011	0.731	0.930	0.960	0.832
	Olomoucine (33 $\mu$ M)	CDK inhibitor	0.697	0.011	0.672	0.772	0.887	0.848
	BAY 11-7085 (0.9 $\mu$ M)	I $\kappa$ B $\alpha$ phosphorylation inhibitor	0.678	0.021	0.641	0.862	0.805	0.631
	BAY 11-7085 (2.8 $\mu$ M)	I $\kappa$ B $\alpha$ phosphorylation inhibitor	0.665	0.021	0.497	0.881	0.871	0.858
	Ro106-9920 (1.8 $\mu$ M)	I $\kappa$ B $\alpha$ ubiquitination inhibitor	0.675	0.021	0.695	0.735	0.611	0.899

secondary activities of test compounds (Berg et al., 2006, 2010; Kunkel et al., 2004a,b).

DMF and MMF were tested in 7 BioMAP® model systems at seven doses starting at 150  $\mu$ M (DMF) or 450  $\mu$ M (MMF) with threefold dilutions. DMF and MMF were active in all 7 BioMAP® systems (Fig. 1). DMF was active between 5.5 and 50  $\mu$ M (IC<sub>50</sub> ~ 30  $\mu$ M) and showed signs of cellular toxicity at 150  $\mu$ M (Fig. 1A). MMF was active between 50 and 150  $\mu$ M (IC<sub>50</sub> ~ 190  $\mu$ M) and was toxic at 450  $\mu$ M (Fig. 1B). DMF and MMF exhibited similar BioMAP® profiles but at distinctly different doses. Mechanistic clustering across multiple doses showed the best correlation between the 16.7  $\mu$ M DMF and 150  $\mu$ M MMF doses (compare Fig. 1A and B) suggesting that the two compounds generate similar responses in these assays, albeit with different potencies. This is highlighted in Fig. 1C, where DMF and MMF are compared directly at 50  $\mu$ M. While direct dose and tissue exposure is difficult to determine, the plasma concentration of MMF falls in a range between 10 and 40  $\mu$ M in vivo after an oral dose of 240 mg DMF (Litjens et al., 2004a,c). BioMAP profiles showed statistically significant inhibition of VCAM-1 and E-selectin (but not ICAM-1) expression, in agreement with findings in psoriasis patients in vivo (Loewe et al., 2001). Additional markers affected by DMF and MMF, which fall outside the 99.7% prediction envelope, included HLA-DR, Eotaxin-3,

CD141/thrombomodulin, CD142/tissue factor, CD40, CD69, IL-1 $\beta$ , M-CSF, IL-8, IP-10, and MIG. The effect of DMF on IL-8, IP-10, and MIG production has been previously reported (Stoof et al., 2001). BioMAP activity profiles across the seven systems were highly reproducible, with a Pearson correlation between the two replicate experiments ranging from 0.83 to 0.95 (Table 2).

Statistical comparison of the DMF and MMF profiles (3C, 4H, LPS, SAg) with the profiles of compounds in the BioSeek database resulted in two types of hits: inhibitors of NF- $\kappa$ B signaling and cyclin-dependent kinase (CDK) inhibitors (Table 3). The NF- $\kappa$ B inhibitor group includes Ro106-9920, BAY 11-7085, and parthenolide. These hits suggest that DMF and MMF inhibit the NF- $\kappa$ B pathway at the level of the NF- $\kappa$ B/I $\kappa$ B complex, in agreement with published studies (Loewe et al., 2001; Vandermeeren et al., 2001). However, the difference in potency between DMF and MMF is profound.

The NF- $\kappa$ B pathway is a pivotal regulator of innate and adaptive immunity, and its dysregulation is implicated in the chronic inflammation of autoimmune diseases. Given the published studies on fumarate modulation of NF- $\kappa$ B signaling (Cross et al., 2011; Gerdes et al., 2007; Ghoreschi et al., 2011; Kim et al., 2010; Lee et al., 2009; Loewe et al., 2001, 2002; Lv et al., 2013; Peng et al., 2012; Vandermeeren et al., 2001) and the differences we saw between potency of DMF and MMF

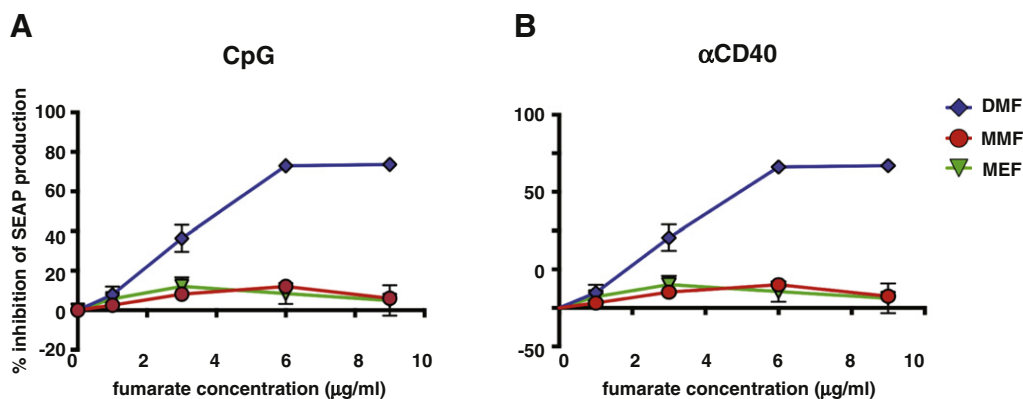


**Fig. 2.** DMF, but not other fumarates, inhibits canonical and non-canonical NF- $\kappa$ B reporter activity in Ramos-Blue cells. Ramos-Blue B cells are a human B cell line that stably expresses an NF- $\kappa$ B/AP-1-inducible secreted alkaline phosphatase (SEAP) reporter gene following stimulation via the NF- $\kappa$ B pathway. Supernatants from Ramos-blue cell cultures were harvested 24 h after stimulation in vitro via TLR9 agonist CpG oligonucleotides ODN 2006 (A) or an agonistic anti-CD40 antibody (B) in the presence of various concentrations of DMSO (vehicle; not shown on graph), DMF (blue diamonds), MMF (red circles), or MEF salt mixture (green inverted triangles) and assayed for alkaline phosphatase activity using a colorimetric enzymatic assay. Relative alkaline phosphatase activity is presented as percent inhibition of alkaline phosphatase activity, calculated vs. vehicle control (DMSO). Graphs depict a representative experiment of 3 independent experiments performed.

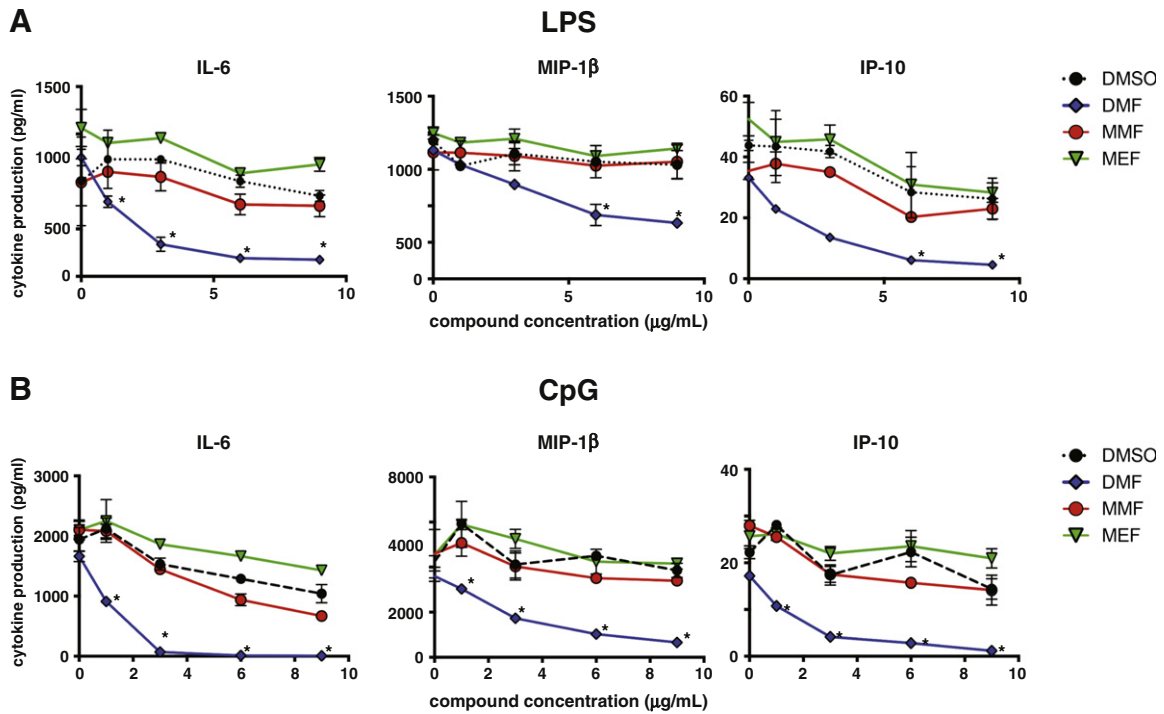


**Fig. 3.** DMF, but not other fumarates, inhibits NF- $\kappa$ B dependent cytokine responses by primary murine splenocytes in vitro. Production of IL-6, IP-10, and MIP-1 $\beta$  by C57BL/6 splenocytes was stimulated in vitro with 10 ng/ml LPS (A) or 10  $\mu$ g/ml CpG B (B) in the presence of DMSO control (black circles), DMF (blue diamonds), MMF (red circles), or MEF mix (green inverted triangles) in DMSO over a range of concentrations (0, 1, 3, 6, and 9  $\mu$ g/ml). Cytokines were measured in cell culture supernatants that were harvested 24 h after stimulation using a Milliplex MAP chemokine/cytokine immunoassay. Statistical significance versus DMSO-treated control is indicated by \* ( $p < 0.05$ ) or \*\* ( $p < 0.01$ ). Graphs depict a representative experiment of a minimum of 3 independent experiments.

in the BioMAP assays, we next performed a detailed analysis of fumarate impacts on NF- $\kappa$ B signaling.

### 3.2 DMF inhibits expression of an NF- $\kappa$ B-responsive reporter gene

DMF has been shown to inhibit NF- $\kappa$ B-mediated cellular responses (Gerdes et al., 2007; Ghoreschi et al., 2011; Kim et al., 2010; Lee et al., 2009; Loewe et al., 2001, 2002; Lv et al., 2013; Peng et al., 2012; Vandermeeren et al., 2001). We sought to determine if MMF or MEF also inhibit NF- $\kappa$ B activity. Ramos-Blue cells, which harbor an NF- $\kappa$ B-inducible secreted embryonic alkaline phosphatase (SEAP) reporter gene, were stimulated with CpG-B or an agonistic anti-CD40 mAb. Toll-like receptor (TLR)9 stimulation (via CpG) activates canonical NF- $\kappa$ B signaling and CD40 agonism activates canonical and non-canonical NF- $\kappa$ B signaling (Kawai and Akira, 2006; Razani et al., 2011; Shih et al., 2011; Sun, 2012). DMF, but not MMF or MEF, inhibited NF- $\kappa$ B reporter activity in a dose-dependent manner under both CpG-B and anti-CD40 stimulation (Fig. 2).

### 3.3 DMF inhibits pro-inflammatory cytokine production by primary murine splenocytes

Having determined that DMF, but not MMF or MEF, significantly inhibited NF- $\kappa$ B activity in a reporter cell line, we next assessed whether these fumarates impacted the production of NF- $\kappa$ B-driven pro-inflammatory cytokines in primary immune cells. Primary splenocytes isolated from C57BL/6 mice were stimulated with LPS or CpG-B in the presence of DMF, MMF, or MEF. Cell culture supernatants were collected at 24 h and IL-6, IP-10, and MIP-1 $\beta$  were assayed. DMF, but not MMF or MEF, significantly reduced the levels of IL-6, IP-10, and MIP-1 $\beta$  after stimulation with LPS (Fig. 3A) or CpG-B (Fig. 3B) in a dose-dependent manner.

### 3.4 DMF inhibits pro-inflammatory cytokine production by human PBMCs

We next wanted to determine if DMF-mediated NF- $\kappa$ B inhibition is consistent between mouse and human primary cells. Freshly isolated human peripheral blood mononuclear cells (PBMC) were stimulated with LPS or CpG-B in the presence of DMF, MMF or MEF. Cell culture supernatants were collected at 24 h and IL-6, IP-10 and MIP-1 $\beta$  were assayed. DMF, but not MMF or MEF, significantly reduced the levels of IL-6, IP-10, and MIP-1 $\beta$  after stimulation with LPS (Fig. 4A) or CpG (Fig. 4B) in a dose-dependent manner. These results demonstrate that the mechanistic impact of DMF on NF- $\kappa$ B-driven pro-inflammatory cytokine production is conserved between mouse and human.

### 3.5 DMF inhibits nuclear translocation of NF- $\kappa$ B signaling subunits p65 and p52

While stimulation of immune cells through TLRs activates canonical NF- $\kappa$ B signaling (Kawai and Akira, 2006), non-canonical NF- $\kappa$ B signaling also plays an important role in immune cell activation (Razani et al., 2011; Sun, 2012). Therefore, we wanted to determine the impact of different fumarates on canonical versus non-canonical NF- $\kappa$ B signaling at the molecular level. Canonical activation of NF- $\kappa$ B is mediated by an I $\kappa$ B kinase (IKK) complex consisting of IKK $\alpha$  and IKK $\beta$  that phosphorylate the inhibitor I $\kappa$ B, resulting in the release of p65/p50 dimers that translocate to the nucleus and stimulate gene transcription at target sites (Shih et al., 2011). Alternatively, activation of NF- $\kappa$ B-inducing kinase (NIK) causes processing of p100, resulting in the release and nuclear translocation of p52/relB dimers (Razani et al., 2011; Sun, 2012).

To determine if DMF directly inhibits NF- $\kappa$ B at the molecular level, we assessed nuclear translocation of the signaling subunits of the canonical (p65) and non-canonical (p52) NF- $\kappa$ B pathway using a high content screen. Human osteosarcoma OS-2 cells were stimulated for 30 min with TNF $\alpha$  (canonical stimulus) or an agonistic lymphotoxin



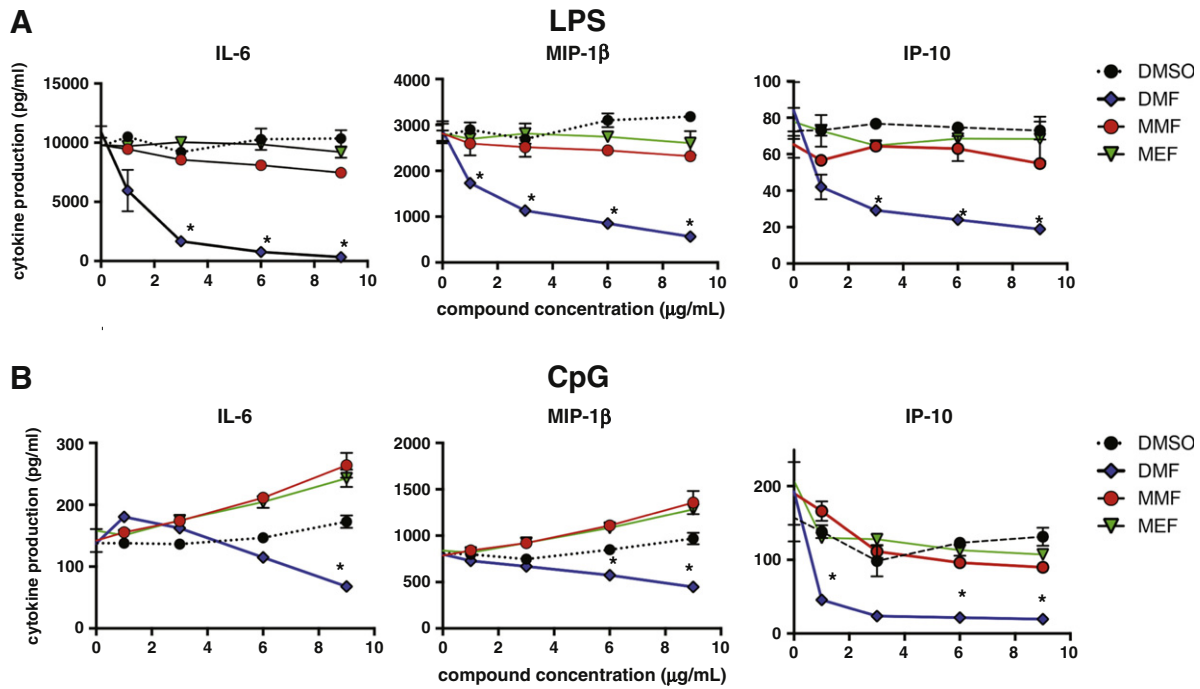


**Fig. 4.** DMF, but not other fumarates, inhibits NF- $\kappa$ B-dependent cytokine responses by primary human PBMC in vitro. Production of IL-6, IP-10, and MIP-1 $\beta$  by Ficoll-purified human PBMC stimulated in vitro with 10 ng/ml LPS (A) or 10  $\mu$ g/ml CpG-B (B) at a standard dose of in the presence of DMSO control (black circles), DMF (blue diamonds), MMF (red circles), or MEF mix (green inverted triangles) in DMSO over a range of concentrations (0, 1, 3, 6, and 9  $\mu$ g/ml). Cytokines were measured in cell culture supernatants that were harvested 24 h after stimulation using a Milliplex MAP chemokine/cytokine immunoassay. Statistical significance versus DMSO-treated control is indicated by \* ( $p < 0.05$ ) or \*\* ( $p < 0.01$ ). Graphs depict a representative experiment of a minimum of 3 independent experiments.

beta-receptor (LT $\beta$ R) antibody (non-canonical stimulus) in the presence of DMF, MMF or MEF. Cells were then fixed, permeabilized, stained for p65 or p52 and imaged. Nuclear translocation was assessed by automated image analysis, and results are shown as percent inhibition based on stimulated DMSO-treated controls. Representative images of p65 translocation (Fig. 5A) and p52 translocation (Fig. 5B) are shown with negative control (unstimulated, DMSO control), positive control (stimulated, DMSO control) and DMF treatment (stimulated, 18  $\mu$ g/ml DMF). DMF, but not MMF or MEF, inhibited p65 and p52 nuclear translocation in a dose-dependent manner (Fig. 5C, D), demonstrating a direct effect on both canonical and non-canonical NF- $\kappa$ B signaling.

### 3.6 DMF inhibition of NF- $\kappa$ B-mediated cytokine release is independent of Nrf2

DMF is able to stimulate the antioxidant response pathway via Nrf2 activation, which may influence pro-inflammatory cytokine production (Lv et al., 2013). There is also experimental evidence of crosstalk between the KEAP1-Nrf2 pathway and NF- $\kappa$ B signaling (Cross et al., 2011; Cuadrado et al., 2014; Ghoreschi et al., 2011; Kim et al., 2010; Lee et al., 2009; Lv et al., 2013; Peng et al., 2012; Yu et al., 2011). Thus, we wanted to determine if the effect of DMF on NF- $\kappa$ B-mediated cytokine production was Nrf2-dependent. Primary splenocytes from WT and Nrf2 $^{-/-}$  mice were stimulated with LPS or a TLR9 agonist, CpG-B for 24 h and cell culture supernatants were assayed for a panel of cytokines. As we previously observed, DMF, but not MMF or MEF, significantly reduced the production of IL-6, IP-10, and MIP-1 $\beta$  in WT C57BL/6 splenocytes in a dose-dependent manner (Fig. 6A–B). The impact of DMF was maintained in splenocytes from Nrf2 $^{-/-}$  mice, demonstrating that the impact of DMF on NF- $\kappa$ B-mediated cytokine production is Nrf2-independent.

In addition to IL-6, IP-10, and MIP-1 $\beta$ , DMF treatment (9  $\mu$ g/ml) led to significant inhibition of numerous other cytokine analytes (Fig. 7). Following LPS stimulation, DMF treatment significantly reduced the production of 13 analytes (G-CSF, GM-CSF, IL-1 $\beta$ , IL-6, IP-10, IL-10, TNF $\alpha$ , MCP-1, MIP-1 $\alpha$ , MIP-1 $\beta$ , MIP2, KC, and RANTES; (all  $p < 0.05$  or

$p < 0.01$ )) by WT splenocytes. In the remaining 12 analytes, 11/12 were below the lowest limit of quantitation. There was reduced production of IL-9 relative to vehicle control; however, this result did not achieve statistical significance ( $p = 0.169$ ).

The ability of DMF to reduce secretion of these cytokines was comparable in both WT (top graph) and Nrf2 $^{-/-}$  (bottom graph) splenocytes (Fig. 7A). DMF treatment significantly reduced production of 16 analytes (G-CSF, GM-CSF, IL-1 $\beta$ , IL-6, IP-10, IL-10, IL-12p70, IL-13, IFN $\gamma$ , TNF $\alpha$ , MCP-1, MIP-1 $\alpha$ , MIP-1 $\beta$ , MIP2, KC, and RANTES; (all  $p < 0.05$  or  $p < 0.01$ )) by Nrf2 $^{-/-}$  splenocytes; in the remaining 9 analytes, 8/9 were below the lowest limit of quantitation. There was reduced production of IL-9 relative to vehicle control; however, this result did not achieve statistical significance ( $p = 0.095$ ).

Following CpG stimulation, DMF treatment significantly reduced the production of 12 analytes (G-CSF, GM-CSF, IL-1 $\alpha$ , IL-1 $\beta$ , IL-6, IL-9, IP-10, KC, MCP-1, MIP-1 $\alpha$ , MIP-1 $\beta$ , and RANTES; (all  $p < 0.05$  or  $p < 0.01$ )) by WT splenocytes. For the remaining 13 analytes, 7/13 were below the lowest limit of quantitation. We observed reduced production of TNF $\alpha$  ( $p = .094$ ), IL-5 ( $p = .087$ ), IL-10 ( $p = .051$ ), IL-12p70 ( $p = 0.101$ ), IL-13 ( $p = 0.214$ ), and IL-15 ( $p = 0.243$ ) relative to vehicle control; however, these results did not achieve statistical significance.

The ability of DMF to reduce secretion of these cytokines in response to CpG stimulation was comparable in both WT (top graph) and Nrf2 $^{-/-}$  (bottom graph) splenocytes (Fig. 7B). DMF treatment significantly reduced production of 15 analytes (GM-CSF, IL-2, IL-5, IL-6, IL-10, IL-12p70, IL-13, IL-15, IP-10, IFN $\gamma$ , KC, MCP-1, MIP-1 $\alpha$ , MIP-1 $\beta$ , and RANTES (all  $p < 0.05$  or  $p < 0.01$ )) by Nrf2 $^{-/-}$  splenocytes; 4 of the remaining 10 analytes were below the lowest limit of quantitation. We observed reduced production of G-CSF ( $p = 0.079$ ), IL-1a ( $p = 0.058$ ), IL-1b ( $p = 0.108$ ), and IL-9 ( $p = 0.095$ ) by DMF-treated versus DMSO-treated Nrf2 $^{-/-}$  splenocytes; however, these results did not achieve statistical significance.

In summary, DMF, but not MMF or MEF, reduced production of a broad range of pro-inflammatory cytokines by LPS- and CpG-stimulated splenocytes in an Nrf2-independent manner.

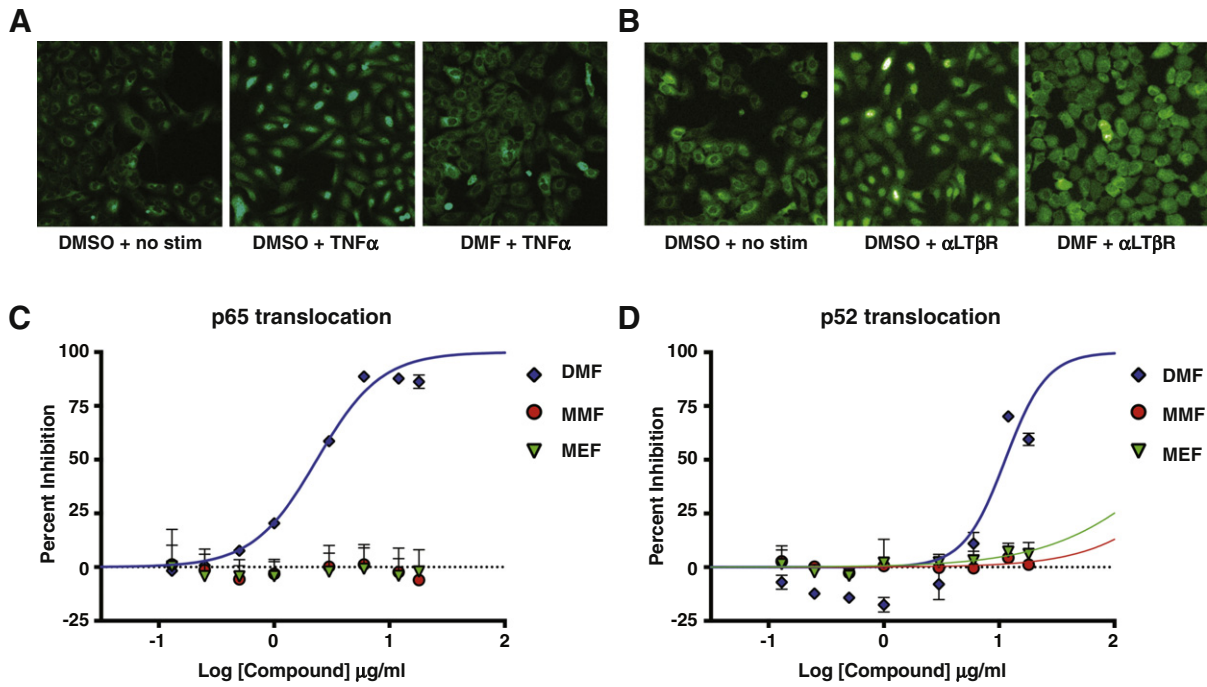


**Fig. 5.** DMF, but not other fumarates, prevents nuclear translocation of NF- $\kappa$ B signaling components following canonical and non-canonical NF- $\kappa$ B stimuli. U-2 OS cells were pre-incubated in vitro with fumarate compounds for 30 min prior to stimulation with 10 ng/ml TNF $\alpha$  (A, B) or 10 ng/ml of an anti-lymphotoxin  $\beta$  receptor ( $\alpha$ LT $\beta$ R) antibody (C, D). Fumarate compounds were tested over a range of eight doses: 0.125, 0.25, 0.5, 1, 3, 6, 12, and 18  $\mu$ g/ml. Four hours after stimulation, the cells were fixed and stained with an antibody that recognizes the p65 protein (A, B) or p52 protein (C, D). Images of each well were acquired on the PerkinElmer Operetta, and the images were analyzed using PerkinElmer Columbus Image Analysis software. Representative images acquired following staining for p65 (A) and p52 (B) in vehicle-treated, unstimulated, vehicle-treated stimulated, and DMF-treated (18  $\mu$ g/ml) stimulated OS-2 cells are shown.

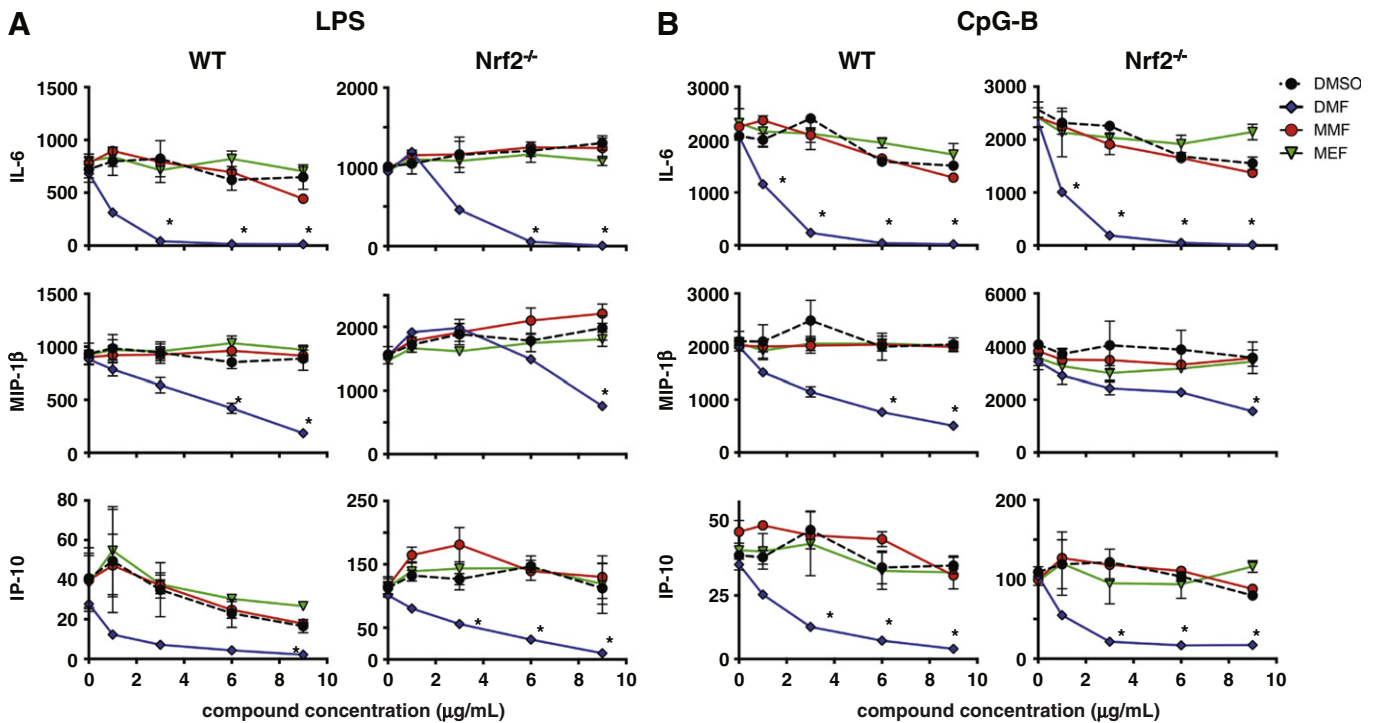


**Fig. 6.** DMF-mediated inhibition of NF- $\kappa$ B-dependent inflammatory cytokine responses is independent of Nrf2. Production of IL-6, IP-10, and MIP-1 $\beta$  by WT and Nrf2<sup>-/-</sup> splenocytes treated with 10 ng/ml of LPS (A) or 10  $\mu$ g/ml CpG-B (B) at a standard dose of in the presence of DMSO control (black circles), DMF (blue diamonds), MMF (red circles), or MEF mix (green inverted triangles) in DMSO over a range of concentrations (0, 1, 3, 6, and 9  $\mu$ g/ml). Cytokines were measured in cell culture supernatants that were harvested 24 h after stimulation using a Milliplex MAP chemokine/cytokine immunoassay. Statistical significance versus DMSO-treated control is indicated by \* ( $p < 0.05$ ) or \*\* ( $p < 0.01$ ). Graphs depict a representative experiment of a minimum of 3 independent experiments.



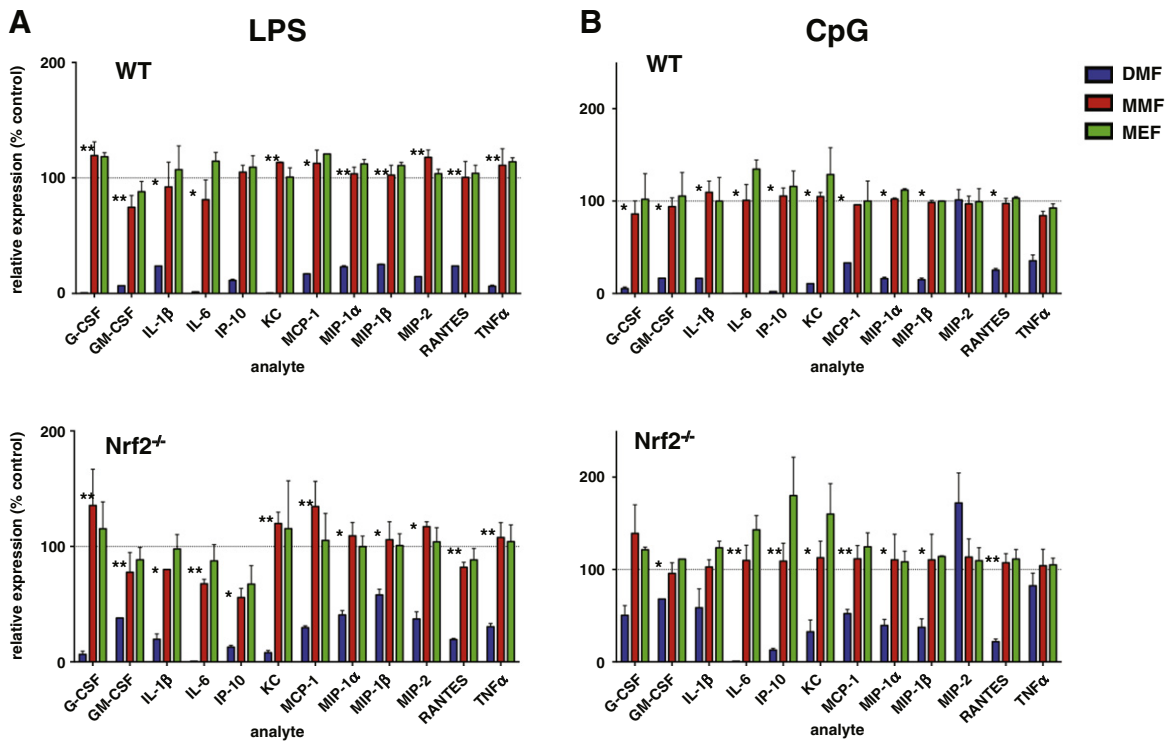


**Fig. 7.** Summary of DMF and other fumarate effects on NF- $\kappa$ B-dependent cytokine responses in both WT and Nrf2<sup>-/-</sup> splenocytes. WT (left column) and Nrf2<sup>-/-</sup> (right column) splenocytes were treated with 10 ng/ml LPS (A) or 10  $\mu$ g/ml CpG-B (B) in the presence of DMSO control (black circles), DMF (blue diamonds), MMF (red circles), or MEF mix (green inverted triangles) in DMSO over a range of concentrations (0, 1, 3, 6, and 9  $\mu$ g/ml). Cytokines were measured in cell culture supernatants that were harvested 24 h after stimulation using a Milliplex MAP chemokine/cytokine immunoassay. Cytokine expression values are represented as the percent production of cytokine vs. DMSO control in splenocytes at the 9  $\mu$ g/ml dose of DMF (blue), MMF (red), or MEF mix (green). Control expression level (100%) is represented by the dotted line. Statistical significance versus DMSO-treated control is indicated by \* ( $p < 0.05$ ) or \*\* ( $p < 0.01$ ). Graphs depict a representative experiment of a minimum of 3 independent experiments.

#### 4. Discussion

It has long been recognized that fumarates are potent therapeutic compounds that exert pleiotropic immunomodulatory effects. Multiple pathways have been implicated in mediating these effects, from strong potentiation of the Nrf2 pathway for cytoprotective and anti-oxidant responses, to the anti-inflammatory effects downstream of HCA2 signaling, to direct inhibition of NF- $\kappa$ B pathway activation. The degree to which each of a variety of individual fumarate esters can impact the involved pathways differentially has yet to be defined, and is complicated by significant variation in the tissue exposure levels, absorption rate, and rate of metabolism for each of the various compounds. DMF, for instance, has highest penetrance in gut, and the vast majority is rapidly transformed *in vivo* by either being metabolized into MMF or by forming conjugates with glutathione. The degree to which each form contributes to the overall immunomodulatory effect *in vivo* is unclear; however, the fact that DMF, MMF, and MEF exhibit differential effects in some models suggests that the differences between these fumarates have significant biological consequences.

In the present study, we investigated the ability of fumarates to modulate a range of cellular pathways. Statistical comparison of the DMF and MMF profiles with profiles of other compounds in the BioSeek Benchmark database showed strong correlation with known inhibitors of NF- $\kappa$ B signaling. These NF- $\kappa$ B inhibitors include Ro106-9920, BAY 11-7085, and parthenolide. Ro106-9920 inhibits phosphorylated I $\kappa$ B $\alpha$  ubiquitination and subsequent degradation, presumably by direct inhibition of an E3 ubiquitin ligase (Lee et al., 2009; Swinney et al., 2002). BAY 11-7085 irreversibly inhibits the phosphorylation of I $\kappa$ B $\alpha$  (Pierce et al., 1997). Parthenolide, a plant-derived sesquiterpene lactone, alkylates the p65 subunit of the NF- $\kappa$ B complex, inhibiting DNA binding (Garcia-Pineres et al., 2004). Parthenolide may also inhibit I $\kappa$ B kinases

through a covalent modification (Kwok et al., 2001). These consistent BioSeek profiles suggest that one of the potential mechanisms of action for DMF and MMF is to inhibit NF- $\kappa$ B pathway at the level of the NF- $\kappa$ B/I $\kappa$ B complex, in agreement with published studies (Loewe et al., 2002; Vandermeeren et al., 2001).

Based on this strong correlation between DMF and MMF and known NF- $\kappa$ B inhibitors, we chose to focus on the ability of various fumarates to modulate NF- $\kappa$ B-driven cellular responses. Dysregulation of the NF- $\kappa$ B pathway is a cardinal feature in the chronic inflammation observed in the context of autoimmune diseases. The results of these studies are quite striking: in all assays, treatment with DMF, but not equivalent doses of MMF or MEF salts, inhibited NF- $\kappa$ B-dependent responses. Treatment with DMF, but not MMF or MEF salts, led to reduced expression of NF- $\kappa$ B-dependent gene activity in a reporter cell line. Treatment of murine or human primary cell cultures with DMF, but not MMF or MEF salts, resulted in significant reduction in cytokine production after stimulation via the canonical and non-canonical NF- $\kappa$ B stimuli, in a dose-dependent fashion. The effect of DMF on NF- $\kappa$ B-dependent responses was confirmed to be a direct effect on NF- $\kappa$ B signaling, as DMF treatment resulted in significant inhibition of the nuclear translocation of the p65 (canonical/classical NF- $\kappa$ B) and p52 (non-canonical NF- $\kappa$ B) signaling in a high content screening assay.

Many of the effects of fumarates have been attributed to the ability of these molecules to stimulate the anti-oxidant response through enhancing the level and activity of the transcription factor Nrf2. Nrf2 activity is regulated at the molecular level by KEAP1. KEAP1 sequesters and poly-ubiquitinates Nrf2 in the cytosol, leading to constitutive degradation (Nguyen et al., 2009). Electrophilic and oxidative stress changes the interaction between Nrf2 and KEAP1, resulting in the stabilization and translocation of Nrf2 to the nucleus. Similarly, DMF interaction with KEAP-1 results in the stabilization and translocation of Nrf2.

There is also a body of literature on the cross-talk between the KEAP1-Nrf2 pathway and NF- $\kappa$ B signaling. Lee et al. demonstrated that KEAP1 binds IKK $\beta$  and mediates ubiquitination and subsequent degradation (Lee et al., 2009). Depletion of KEAP1 led to an increase in NF- $\kappa$ B signaling. A separate study demonstrated that genetic knockdown of KEAP1 led to enhanced IL-6 production, an NF- $\kappa$ B target gene, in LPS-stimulated macrophages. Interestingly, we demonstrate in our study that DMF treatment inhibited pro-inflammatory cytokine production by cultured WT and Nrf2<sup>-/-</sup> splenocytes with equal efficiency, demonstrating that the ability of DMF to suppress NF- $\kappa$ B dependent responses was independent of Nrf2 activity.

These results demonstrate that equivalent amounts of DMF, MMF, and MEF salts display distinct abilities to influence immune responses via the NF- $\kappa$ B pathway in these assays. As mentioned previously, DMF is rapidly metabolized to MMF (its primary metabolite) and also forms glutathione adjuncts. Based on the metabolism and pharmacokinetics of DMF it is impossible to know the *in vivo* targets and local tissue exposure to DMF. The assumption has been that significant direct exposure to unmodified/unmetabolized DMF is limited to a small population of cells and that consequently, the therapeutic effects of DMF are mediated by its primary metabolite MMF. As a consequence, preclinical studies have traditionally used DMF and MMF interchangeably both *in vitro* and *in vivo*. However, this assumption is flawed, as the tissue concentration and target cell exposure to MMF *in vivo* is not known, and therefore it is difficult to draw meaningful parallels between *in vitro* and *in vivo* active concentration for MMF. In the absence of known MMF target tissue concentrations for modeling the effects of fumarates, we based the range of concentrations used in our NF- $\kappa$ B-driven assays on the reported concentration range for MMF in the plasma of patients, where MMF concentration has been measured in a range from 1 to 5  $\mu$ g/mL ( $\approx$  10–40  $\mu$ M) (Litjens et al., 2004a; Sheikh et al., 2013). The highest dose we used in our cytokine production assays, 9  $\mu$ g/mL, corresponds to an approximate concentration of 60  $\mu$ M for DMF and 70  $\mu$ M for MMF. Based on the assumption that the range of concentrations used approximates the plasma concentration of MMF in patients, the differential fumarate effects on NF- $\kappa$ B activity observed may well represent effects at a more “physiological” concentration. The BioSeek profiles for DMF and MMF indicate that these concentrations fall well below toxicity level for both compounds but reflect a significant difference in potency between the two compounds for modifying NF- $\kappa$ B-driven responses, as DMF had an IC<sub>50</sub> of approximately 30  $\mu$ M versus 190  $\mu$ M for MMF. The pharmacokinetics and serum concentration of MEFs *in vivo* is similar to that of MMF, not DMF, so at similarly “physiological” concentrations of MEFs, we did not observe any inhibition of NF- $\kappa$ B-driven responses. That we did not observe any significant effect of MMF or MEF on NF- $\kappa$ B-driven responses at these levels suggests that perhaps a significant component of the therapeutic benefit of fumarates is mediated by effects on cells and tissues that either have direct exposure to DMF or experience very high local concentrations of MMF and MEF.

In this study, we have directly compared the activity of DMF and MMF. We observed significant differences between the biological activities of these two closely related, yet distinct compounds. In addition, the inclusion of MEF salts without DMF also allowed us to separate the activity of MEF salts on NF- $\kappa$ B-driven cytokine production from those mediated by DMF. These results establish that DMF is the most potent fumarate tested for modulating NF- $\kappa$ B signaling. The differential effects we observed on NF- $\kappa$ B-dependent responses were largely Nrf2-independent, despite the well-established role for Nrf2 in fumarate-mediated cellular responses. This suggests that the impact that fumarates exert on cellular responses is mediated by the integration of their effects on multiple and distinct pathways, each of which may be differentially affected depending on which fumarate is present. While DMF may be more effective than MMF or MEF salts at modulating NF- $\kappa$ B-driven responses, as these data indicate, the activation of Nrf2, the modulation of the glutathione system, or the activation of GPR109A may all be mediated differentially depending on whether the cells

have been exposed to DMF, MMF, or MEF salts. In that vein, it is important to note that MMF is a significantly more potent activator of the HCA2 pathway (70 nM) than DMF (> 10  $\mu$ M) (Tang et al., 2008), and that concentration of MMF falls well within the plasma exposure levels for MMF observed after patients receive a 240 mg dose of delayed-release DMF (C<sub>max</sub> of 1–3  $\mu$ g/mL MMF in plasma) (Sheikh et al., 2013). Given the common pharmacodynamic observation of flushing in delayed-release DMF clinical trials (Fox, 2012; Fox et al., 2014; Gold, 2011; Kappos et al., 2008, 2012), and the role of HCA2 in mediating these responses (Hanson et al., 2010, 2012), it seems likely that there is activation of this receptor in patients taking delayed-release DMF. Although MMF and MEF were not active in modulating inflammatory NF- $\kappa$ B-related responses in the assays described here, given the emerging role of HCA2 in regulating macrophage function it is likely that MMF and MEF exert other immunomodulatory activities that need to be more fully explored (Chen et al., 2014; Hanson et al., 2010, 2012; Tang et al., 2008).

Additional studies will be necessary to further explore potential differential effects of these compounds and identify their relative contributions to the various biological activities attributed to fumarates. Understanding how each fumarate impacts these various biological pathways relative to one another will be crucial to understanding the contributions these compounds make to the therapeutic effects observed in patients.

Supplementary data to this article can be found online at <http://dx.doi.org/10.1016/j.jneuroim.2015.04.006>.

## Disclosures

This research was supported by Biogen. All authors are employees of and hold stock/stock options in Biogen.

## References

- Albrecht, P., Bouchachia, I., Goebels, N., Henke, N., Hofstetter, H.H., Issberner, A., Kovacs, Z., Lewerenz, J., Lisak, D., Maher, P., et al., 2012. Effects of dimethyl fumarate on neuroprotection and immunomodulation. *J. Neuroinflammation* 9, 163.
- Berg, E.L., Kunkel, E.J., Hytopoulos, E., Plavec, I., 2006. Characterization of compound mechanisms and secondary activities by BioMAP analysis. *J. Pharmacol. Toxicol. Methods* 53, 67–74.
- Berg, E.L., Yang, J., Melrose, J., Nguyen, D., Privat, S., Rosler, E., Kunkel, E.J., Ekins, S., 2010. Chemical target and pathway toxicity mechanisms defined in primary human cell systems. *J. Pharmacol. Toxicol. Methods* 61, 3–15.
- Chen, H., Assmann, J.C., Krenz, A., Rahman, M., Grimm, M., Karsten, C.M., Kohl, J., Offermanns, S., Wettschureck, N., Schwaninger, M., 2014. Hydroxycarboxylic acid receptor 2 mediates dimethyl fumarate's protective effect in EAE. *J. Clin. Invest.* 124, 2188–2192.
- Cross, S.A., Cook, D.R., Chi, A.W., Vance, P.J., Kolson, L.L., Wong, B.J., Jordan-Sciutto, K.L., Kolson, D.L., 2011. Dimethyl fumarate, an immune modulator and inducer of the antioxidant response, suppresses HIV replication and macrophage-mediated neurotoxicity: a novel candidate for HIV neuroprotection. *J. Immunol.* 187, 5015–5025.
- Cuadrado, A., Martin-Moldes, Z., Ye, J., Lastres-Becker, I., 2014. Transcription factors NRF2 and NF-kappaB are coordinated effectors of the Rho family, GTP-binding protein RAC1 during inflammation. *J. Biol. Chem.* 289, 15244–15258.
- Dibbert, S., Clement, B., Skak-Nielsen, T., Mrowietz, U., Rostami-Yazdi, M., 2013. Detection of fumarate–glutathione adducts in the portal vein blood of rats: evidence for rapid dimethylfumarate metabolism. *Arch. Dermatol. Res.* 305, 447–451.
- Digby, J.E., Martinez, F., Jefferson, A., Ruparelia, N., Chai, J., Wamil, M., Greaves, D.R., Choudhury, R.P., 2012. Anti-inflammatory effects of nicotinic acid in human monocytes are mediated by GPR109A dependent mechanisms. *Arterioscler. Thromb. Vasc. Biol.* 32, 669–676.
- Fox, R., 2012. The New England Journal of Medicine publishes pivotal data demonstrating efficacy and safety of oral BG-12 (dimethyl fumarate) in multiple sclerosis. *Can. J. Neurosci. Nurs.* 34, 7–11.
- Fox, R.J., Miller, D.H., Phillips, J.T., Hutchinson, M., Havrdova, E., Kita, M., Yang, M., Raghupathi, K., Novas, M., Sweetser, M.T., Vigiotta, V., Dawson, K.T., 2012. CONFIRM Study Investigators. Placebo-controlled phase 3 study of oral BG-12 or glatiramer in multiple sclerosis. *N. Engl. J. Med.* 367 (12), 1087–1097.
- Fox, R.J., Kita, M., Cohan, S.L., Henson, L.J., Zambrano, J., Scannevin, R.H., O’Gorman, J., Novas, M., Dawson, K.T., Phillips, J.T., 2014. BG-12 (dimethyl fumarate): a review of mechanism of action, efficacy, and safety. *Curr. Med. Res. Opin.* 30, 251–262.
- Garcia-Pineres, A.J., Lindenmeyer, M.T., Merfort, I., 2004. Role of cysteine residues of p65/NF-kappaB on the inhibition by the sesquiterpene lactone parthenolide and N-ethyl maleimide, and on its transactivating potential. *Life Sci.* 75, 841–856.

- Gerdes, S., Shakeri, K., Mrowietz, U., 2007. Dimethylfumarate inhibits nuclear binding of nuclear factor kappaB but not of nuclear factor of activated T cells and CCAAT/enhancer binding protein beta in activated human T cells. *Br. J. Dermatol.* 156, 838–842.
- Ghashghaieina, M., Bobbala, D., Wieder, T., Koka, S., Bruck, J., Fehrenbacher, B., Rocken, M., Schaller, M., Lang, F., Ghoreschi, K., 2010. Targeting glutathione by dimethylfumarate protects against experimental malaria by enhancing erythrocyte cell membrane scrambling. *Am. J. Physiol. Cell Physiol.* 299, C791–C804.
- Ghoreschi, K., Bruck, J., Kellerer, C., Deng, C., Peng, H., Rothfuss, O., Hussain, R.Z., Gocke, A.R., Respa, A., Glucocova, I., et al., 2011. Fumarates improve psoriasis and multiple sclerosis by inducing type II dendritic cells. *J. Exp. Med.* 208, 2291–2303.
- Gold, R., 2011. Oral therapies for multiple sclerosis: a review of agents in phase III development or recently approved. *CNS Drugs* 25, 37–52.
- Gold, R., Kappos, L., Arnold, D.L., Bar-Or, A., Giovannoni, G., Selmaj, K., Tornatore, C., Sweetser, M.T., Yang, M., Sheikh, S.I., Dawson, K.T., 2012a. DEFINE Study Investigators. Placebo-controlled phase 3 study of oral BG-12 for relapsing multiple sclerosis. *N Engl J Med.* 367 (12), 1098–1107.
- Gold, R., Linker, R.A., Stangel, M., 2012b. Fumaric acid and its esters: an emerging treatment for multiple sclerosis with antioxidative mechanism of action. *Clin. Immunol.* 142, 44–48.
- Hanson, J., Gille, A., Zwykiel, S., Lukasova, M., Clausen, B.E., Ahmed, K., Tunaru, S., Wirth, A., Offermanns, S., 2010. Nicotinic acid- and monomethyl fumarate-induced flushing involves GPR109A expressed by keratinocytes and COX-2-dependent prostanoic acid formation in mice. *J. Clin. Invest.* 120, 2910–2919.
- Hanson, J., Gille, A., Offermanns, S., 2012. Role of HCA(2) (GPR109A) in nicotinic acid and fumaric acid ester-induced effects on the skin. *Pharmacol. Ther.* 136, 1–7.
- Hoefnagel, J.J., Thio, H.B., Willemze, R., Bouwes Bavinck, J.N., 2003. Long-term safety aspects of systemic therapy with fumaric acid esters in severe psoriasis. *Br. J. Dermatol.* 149, 363–369.
- Kappos, L., Gold, R., Miller, D.H., MacManus, D.G., Havrdova, E., Limmroth, V., Polman, C.H., Schmierer, K., Youstry, T.A., Yang, M., et al., 2008. Efficacy and safety of oral fumarate in patients with relapsing–remitting multiple sclerosis: a multicentre, randomised, double-blind, placebo-controlled phase IIb study. *Lancet* 372, 1463–1472.
- Kappos, L., Gold, R., Miller, D.H., MacManus, D.G., Havrdova, E., Limmroth, V., Polman, C.H., Schmierer, K., Youstry, T.A., Eraksoy, M., et al., 2012. Effect of BG-12 on contrast-enhanced lesions in patients with relapsing–remitting multiple sclerosis: subgroup analyses from the phase 2b study. *Mult. Scler.* 18, 314–321.
- Kawai, T., Akira, S., 2006. TLR signaling. *Cell Death Differ.* 13, 816–825.
- Kim, J.E., You, D.J., Lee, C., Ahn, C., Seong, J.Y., Hwang, J.I., 2010. Suppression of NF-kappaB signaling by KEAP1 regulation of IKKbeta activity through autophagic degradation and inhibition of phosphorylation. *Cell. Signal.* 22, 1645–1654.
- Kunkel, E.J., Dea, M., Ebens, A., Hytopoulos, E., Melrose, J., Nguyen, D., Ota, K.S., Plavec, I., Wang, Y., Watson, S.R., et al., 2004a. An integrative biology approach for analysis of drug action in models of human vascular inflammation. *FASEB J.* 18, 1279–1281.
- Kunkel, E.J., Plavec, I., Nguyen, D., Melrose, J., Rosler, E.S., Kao, L.T., Wang, Y., Hytopoulos, E., Bishop, A.C., Bateman, R., et al., 2004b. Rapid structure-activity and selectivity analysis of kinase inhibitors by BioMAP analysis in complex human primary cell-based models. *Assay Drug Dev. Technol.* 2, 431–441.
- Kwok, B.H., Koh, B., Ndubuisi, M.I., Elofsson, M., Crews, C.M., 2001. The anti-inflammatory natural product parthenolide from the medicinal herb Feverfew directly binds to and inhibits IkkappaB kinase. *Chem. Biol.* 8, 759–766.
- Lee, D.F., Kuo, H.P., Liu, M., Chou, C.K., Xia, W., Du, Y., Shen, J., Chen, C.T., Huo, L., Hsu, M.C., et al., 2009. KEAP1 E3 ligase-mediated downregulation of NF-kappaB signaling by targeting IKKbeta. *Mol. Cell* 36, 131–140.
- Lehmann, J.C., Listopad, J.J., Rentzsch, C.U., Igney, F.H., von Bonin, A., Hennekes, H.H., Asadullah, K., Docke, W.D., 2007. Dimethylfumarate induces immunosuppression via glutathione depletion and subsequent induction of heme oxygenase 1. *J. Invest. Dermatol.* 127, 835–845.
- Linker, R.A., Gold, R., 2013. Dimethyl fumarate for treatment of multiple sclerosis: mechanism of action, effectiveness, and side effects. *Curr. Neurol. Neurosci. Rep.* 13, 394.
- Linker, R.A., Lee, D.H., Stangel, M., Gold, R., 2008. Fumarates for the treatment of multiple sclerosis: potential mechanisms of action and clinical studies. *Expert. Rev. Neurother.* 8, 1683–1690.
- Linker, R.A., Lee, D.H., Ryan, S., van Dam, A.M., Conrad, R., Bista, P., Zeng, W., Hronowsky, X., Buko, A., Chollate, S., et al., 2011. Fumaric acid esters exert neuroprotective effects in neuroinflammation via activation of the Nrf2 antioxidant pathway. *Brain* 134, 678–692.
- Litjens, N.H., Burggraaf, J., van Strijen, E., van Gulpen, C., Mattie, H., Schoemaker, R.C., van Dissel, J.T., Thio, H.B., Nibbering, P.H., 2004a. Pharmacokinetics of oral fumarates in healthy subjects. *Br. J. Clin. Pharmacol.* 58, 429–432.
- Litjens, N.H., Rademaker, M., Ravensbergen, B., Rea, D., van der Plas, M.J., Thio, B., Walding, A., van Dissel, J.T., Nibbering, P.H., 2004b. Monomethylfumarate affects polarization of monocyte-derived dendritic cells resulting in down-regulated Th1 lymphocyte responses. *Eur. J. Immunol.* 34, 565–575.
- Litjens, N.H., van Strijen, E., van Gulpen, C., Mattie, H., van Dissel, J.T., Thio, H.B., Nibbering, P.H., 2004c. In vitro pharmacokinetics of anti-psoriatic fumaric acid esters. *BMC Pharmacol.* 4, 22.
- Litjens, N.H., Rademaker, M., Ravensbergen, B., Thio, H.B., van Dissel, J.T., Nibbering, P.H., 2006. Effects of monomethylfumarate on dendritic cell differentiation. *Br. J. Dermatol.* 154, 211–217.
- Loewe, R., Pillinger, M., de Martin, R., Mrowietz, U., Groger, M., Holthoner, W., Wolff, K., Wiegrebe, W., Jirovsky, D., Petzelbauer, P., 2001. Dimethylfumarate inhibits tumor-necrosis-factor-induced CD62E expression in an NF-kappa B-dependent manner. *J. Invest. Dermatol.* 117, 1363–1368.
- Loewe, R., Holthoner, W., Groger, M., Pillinger, M., Gruber, F., Mechtcheriakova, D., Hofer, E., Wolff, K., Petzelbauer, P., 2002. Dimethylfumarate inhibits TNF-induced nuclear entry of NF-kappa B/p65 in human endothelial cells. *J. Immunol.* 168, 4781–4787.
- Lv, P., Xue, P., Dong, J., Peng, H., Clewell, R., Wang, A., Wang, Y., Peng, S., Qu, W., Zhang, Q., et al., 2013. Keap1 silencing boosts lipopolysaccharide-induced transcription of interleukin 6 via activation of nuclear factor kappaB in macrophages. *Toxicol. Appl. Pharmacol.* 272, 697–702.
- MacManus, D.G., Miller, D.H., Kappos, L., Gold, R., Havrdova, E., Limmroth, V., Polman, C.H., Schmierer, K., Youstry, T.A., Eraksoy, M., et al., 2011. BG-12 reduces evolution of new enhancing lesions to T1-hypointense lesions in patients with multiple sclerosis. *J. Neurol.* 258, 449–456.
- Moed, H., Stooft, T.J., Boersma, D.M., von Blomberg, B.M., Gibbs, S., Bruynzeel, D.P., Scheper, R.J., Rustemeyer, T., 2004. Identification of anti-inflammatory drugs according to their capacity to suppress type-1 and type-2 T cell profiles. *Clin. Exp. Allergy* 34, 1868–1875.
- Moharreggh-Khiabani, D., Linker, R.A., Gold, R., Stangel, M., 2009. Fumaric Acid and its esters: an emerging treatment for multiple sclerosis. *Curr. Neuropharmacol.* 7, 60–64.
- Mrowietz, U., Asadullah, K., 2005. Dimethylfumarate for psoriasis: more than a dietary curiosity. *Trends Mol. Med.* 11, 43–48.
- Murphy, T.H., Yu, J., Ng, R., Johnson, D.A., Shen, H., Honey, C.R., Johnson, J.A., 2001. Preferential expression of antioxidant response element mediated gene expression in astrocytes. *J. Neurochem.* 76, 1670–1678.
- Nelson, K.C., Carlson, J.L., Newman, M.L., Sternberg Jr., P., Jones, D.P., Kavanagh, T.J., Diaz, D., Cai, J., Wu, M., 1999. Effect of dietary inducer dimethylfumarate on glutathione in cultured human retinal pigment epithelial cells. *Invest. Ophthalmol. Vis. Sci.* 40, 1927–1935.
- Nguyen, T., Nioi, P., Pickett, C.B., 2009. The Nrf2-antioxidant response element signaling pathway and its activation by oxidative stress. *J. Biol. Chem.* 284, 13291–13295.
- Peng, H., Guerau-de-Arellano, M., Mehta, V.B., Yang, Y., Huss, D.J., Papenfuss, T.L., Lovett-Racke, A.E., Racke, M.K., 2012. Dimethyl fumarate inhibits dendritic cell maturation via nuclear factor kappaB (NF-kappaB) and extracellular signal-regulated kinase 1 and 2 (ERK1/2) and mitogen stress-activated kinase 1 (MSK1) signaling. *J. Biol. Chem.* 287, 28017–28026.
- Peterson, J.D., Herzenberg, L.A., Vasquez, K., Waltenbaugh, C., 1998. Glutathione levels in antigen-presenting cells modulate Th1 versus Th2 response patterns. *Proc. Natl. Acad. Sci. U. S. A.* 95, 3071–3076.
- Pierce, J.W., Schoenleber, R., Jesmok, G., Best, J., Moore, S.A., Collins, T., Gerritsen, M.E., 1997. Novel inhibitors of cytokine-induced IkkappaBalpha phosphorylation and endothelial cell adhesion molecule expression show anti-inflammatory effects in vivo. *J. Biol. Chem.* 272, 21096–21103.
- Rahman, M., Muhammad, S., Khan, M.A., Chen, H., Ridder, D.A., Muller-Fielitz, H., Pokorna, B., Vollbrandt, T., Stolting, I., Nadrowitz, R., et al., 2014. The beta-hydroxybutyrate receptor HCA2 activates a neuroprotective subset of macrophages. *Nat. Commun.* 5, 3944.
- Razani, B., Reichardt, A.D., Cheng, G., 2011. Non-canonical NF-kappaB signaling activation and regulation: principles and perspectives. *Immunol. Rev.* 244, 44–54.
- Reick, C., Ellrichmann, G., Thone, J., Scannevin, R.H., Saft, C., Linker, R.A., Gold, R., 2014. Neuroprotective dimethyl fumarate synergizes with immunomodulatory interferon beta to provide enhanced axon protection in autoimmune neuroinflammation. *Exp. Neurol.* 257, 50–56.
- Roll, A., Reich, K., Boer, A., 2007. Use of fumaric acid esters in psoriasis. *Indian J. Dermatol. Venereol. Leprol.* 73, 133–137.
- Rostami Yazdi, M., Mrowietz, U., 2008. Fumaric acid esters. *Clin. Dermatol.* 26, 522–526.
- Rostami-Yazdi, M., Clement, B., Schmidt, T.J., Schinor, D., Mrowietz, U., 2009. Detection of metabolites of fumaric acid esters in human urine: implications for their mode of action. *J. Invest. Dermatol.* 129, 231–234.
- Rostami-Yazdi, M., Clement, B., Mrowietz, U., 2010. Pharmacokinetics of anti-psoriatic fumaric acid esters in psoriasis patients. *Arch. Dermatol. Res.* 302, 531–538.
- Scannevin, R.H., Chollate, S., Jung, M.Y., Shackett, M., Patel, H., Bista, P., Zeng, W., Ryan, S., Yamamoto, M., Lukashov, M., Rhodes, K.J., 2012. Fumarates promote cytoprotection of central nervous system cells against oxidative stress via the nuclear factor (erythroid-derived 2)-like 2 pathway. *J. Pharmacol. Exp. Ther.* 341, 274–284.
- Schilling, S., Goelz, S., Linker, R., Luehder, F., Gold, R., 2006. Fumaric acid esters are effective in chronic experimental autoimmune encephalomyelitis and suppress macrophage infiltration. *Clin. Exp. Immunol.* 145, 101–107.
- Schmidt, M.M., Dringen, R., 2010. Fumaric acid diesters deprive cultured primary astrocytes rapidly of glutathione. *Neurochem. Int.* 57, 460–467.
- Schmidt, T.J., Ak, M., Mrowietz, U., 2007. Reactivity of dimethyl fumarate and methylhydrogen fumarate towards glutathione and N-acetyl-L-cysteine-preparation of S-substituted thiosuccinic acid esters. *Bioorg. Med. Chem.* 15, 333–342.
- Sheikh, S.I., Nestorov, I., Russell, H., O'Gorman, J., Huang, R., Milne, G.L., Scannevin, R.H., Novas, M., Dawson, K.T., 2013. Tolerability and pharmacokinetics of delayed-release dimethyl fumarate administered with and without aspirin in healthy volunteers. *Clin. Ther.* 35, 1582–1594 (e1589).
- Shih, V.F., Tsui, R., Caldwell, A., Hoffmann, A., 2011. A single NFkappaB system for both canonical and non-canonical signaling. *Cell Res.* 21, 86–102.
- Spencer, S.R., Wilczak, C.A., Talalay, P., 1990. Induction of glutathione transferases and NAD(P)H:quinone reductase by fumaric acid derivatives in rodent cells and tissues. *Cancer Res.* 50, 7871–7875.
- Stooft, T.J., Flier, J., Sampat, S., Nieboer, C., Tensen, C.P., Boersma, D.M., 2001. The anti-psoriatic drug dimethylfumarate strongly suppresses chemokine production in human keratinocytes and peripheral blood mononuclear cells. *Br. J. Dermatol.* 144, 1114–1120.
- Sun, S.C., 2012. The noncanonical NF-kappaB pathway. *Immunol. Rev.* 246, 125–140.
- Swinney, D.C., Xu, Y.Z., Scarafia, L.E., Lee, I., Mak, A.Y., Gan, Q.F., Ramesha, C.S., Mulkins, M.A., Dunn, J., So, O.Y., et al., 2002. A small molecule ubiquitination inhibitor blocks NF-kappa B-dependent cytokine expression in cells and rats. *J. Biol. Chem.* 277, 23573–23581.
- Tang, H., Lu, J.Y., Zheng, X., Yang, Y., Reagan, J.D., 2008. The psoriasis drug monomethylfumarate is a potent nicotinic acid receptor agonist. *Biochem. Biophys. Res. Commun.* 375, 562–565.

- Vandermeeren, M., Janssens, S., Borgers, M., Geysen, J., 1997. Dimethylfumarate is an inhibitor of cytokine-induced E-selectin, VCAM-1, and ICAM-1 expression in human endothelial cells. *Biochem. Biophys. Res. Commun.* 234, 19–23.
- Vandermeeren, M., Janssens, S., Wouters, H., Borghmans, I., Borgers, M., Beyaert, R., Geysen, J., 2001. Dimethylfumarate is an inhibitor of cytokine-induced nuclear translocation of NF-kappa B1, but not RelA in normal human dermal fibroblast cells. *J. Invest. Dermatol.* 116, 124–130.
- Werdenberg, D., Joshi, R., Wolfram, S., Merkle, H.P., Langguth, P., 2003. Presystemic metabolism and intestinal absorption of antipsoriatic fumaric acid esters. *Biopharm. Drug Dispos.* 24, 259–273.
- Wilms, H., Sievers, J., Rickert, U., Rostami-Yazdi, M., Mrowietz, U., Lucius, R., 2010. Dimethylfumarate inhibits microglial and astrocytic inflammation by suppressing the synthesis of nitric oxide, IL-1beta, TNF-alpha and IL-6 in an in-vitro model of brain inflammation. *J. Neuroinflammation* 7, 30.
- Yu, M., Li, H., Liu, Q., Liu, F., Tang, L., Li, C., Yuan, Y., Zhan, Y., Xu, W., Li, W., et al., 2011. Nuclear factor p65 interacts with Keap1 to repress the Nrf2-ARE pathway. *Cell. Signal.* 23, 883–892.